ARTICLES

Synthesis of Metal Alloy Nanoparticles in Solution by Laser Irradiation of a Metal Powder Suspension

Jin Zhang, Jessica Worley, Stephane Dénommée, Christopher Kingston, Zygmunt J. Jakubek, Yves Deslandes, Michael Post, and Benoit Simard*

National Research Council of Canada, 100 Sussex Drive, Ottawa, Ontario K1A 0R6, Canada

Nadi Braidy and Gianluigi A. Botton

Materials Science and Engineering, Brockhouse Institute of Materials Research, McMaster University, 1280 Main Street West, Hamilton, Ontario L8S 4L7, Canada

Received: August 6, 2002; In Final Form: January 24, 2003

A simple, convenient, and general method for the synthesis of metal and metal alloy nanoparticles is presented. Irradiation of metal powders in suspension in either aqueous or organic solutions by unfocused 532 nm laser radiation produces nanoparticles with a homogeneous composition proportional to the composition of the starting metal powder mixture. This is demonstrated using UV−vis absorption spectroscopy, transmission electron microscopy, energy-dispersive X-ray spectroscopy, and modelization. The mechanism of alloy formation is discussed.

I. Introduction

Properties of nanoparticles are determined by their shapes, sizes, and chemical environments.[1−4] Therefore, they can be used to design extremely sensitive and specific biological, chemical, and environmental sensors.[1−3,5] It is generally agreed that nanoparticle-based detection will displace dye-based and chemical methods within the next 10 years. It is therefore imperative that new versatile methods for nanoparticle synthesis be developed. The sensitivity and specificity of metal nanoparticle detection has been recently demonstrated by Kim et al. for environmental applications[5] and by Mirkin et al. for biological applications.[6−10] These methods are based on the use of gold, silver, or silver-coated gold nanoparticles. It may become advantageous to use alloys or mixtures of metals or simply metals other than coinage metals in many applications. This would definitely be the case in applications where the nanoparticles act as catalysts. This would also be the case in applications where the magnetic properties of the nanoparticles are used to probe chemical or biological events or where thiol chemistry is not appropriate. Finally, if the optical properties are used, it may be advantageous to tune the absorption feature to specific wavelength ranges.

Unfortunately, there exist no rapid and versatile methods to synthesize metal or metal alloy nanoparticles. Laser vaporization of a solid target previously prepared offers the possibility of preparing nanoparticles of all kinds, including alloys and mixtures, but the technique suffers from low yields; that is to say, it is difficult to build up sufficient concentrations for applications.[11−19] Another method, recently demonstrated by Chen et al., is based on laser irradiation ($\lambda = 532$ nm) of a mixture of previously prepared monometallic colloidal solutions to produce alloy nanoparticles.[20−21] The major disadvantage of this technique is that the colloidal solutions must be prepared prior to irradiation, which limits the number of potential solvents drastically. Building on this report and on a previous report by Yeh et al. that Cu nanoparticles can be prepared from CuO powder,[22] we hypothesized that laser irradiation of mixtures of micrometer-sized metal powders should lead to the formation of alloy nanoparticles. We further hypothesized that this could be done in organic as well as aqueous solutions. In this paper we report on the validation of this hypothesis and demonstrate the versatility and easy application of the method using Ag−Au alloy nanoparticles.

II. Experimental Section

The method consists of irradiating a heterogeneous suspension of the required metal powders dispersed in a solvent of choice with an unfocused laser beam. With the laser operating at 532 nm, the threshold fluence has been determined to be equal to 5−10 (mJ/cm^2)/pulse. The rate at which nanoparticles are formed and the size distribution depend on the laser fluence as well as the nature of the solvent and the stabilizing agent. Details of the dependence are presently under investigation. Wavelengths other than 532 nm can also be used but, in general, with UV or IR beams photodecomposition or rapid heating, respectively, of a solvent or a stabilizer may take place.

In the present experiment the Ag−Au nanoparticles were produced by laser irradiation of heterogeneous suspensions of Ag (Alfa Aesar, APS 0.5−1 μm, 99.9%) and Au (Alfa Aesar,

* To whom correspondence should be addressed. E-mail: Benoit.Simard@nrc.ca.

10.1021/jp027269k CCC: $25.00
Published on Web 06/27/2003

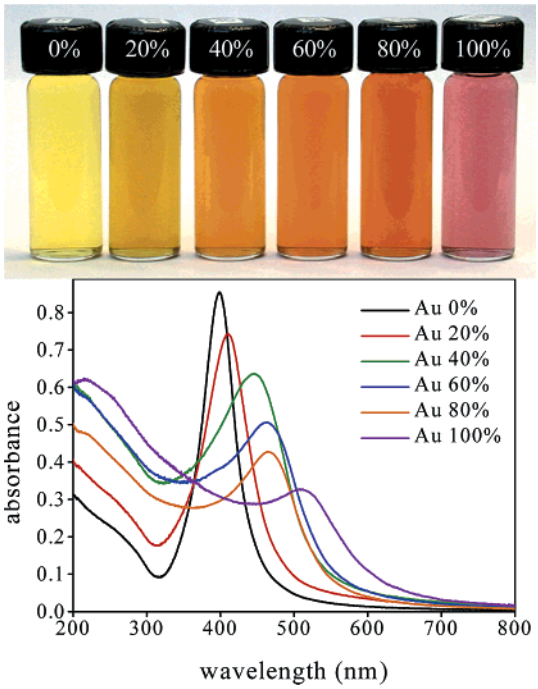

Figure 1. A photograph (top panel) and the corresponding UV−vis extinction spectra (bottom panel) of a series of diluted colloids of Ag−Au nanoparticles (set 2) with increasing Au mole fraction (shown in each panel).

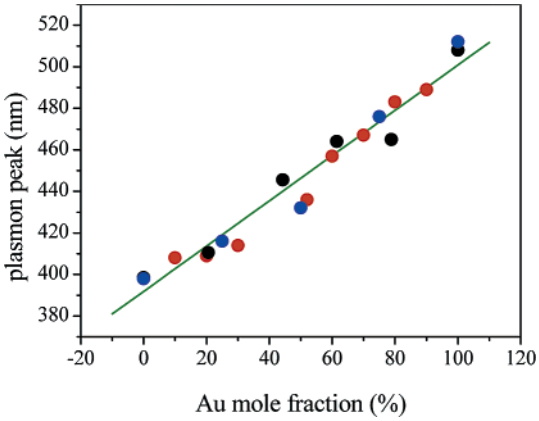

Figure 2. Plasmon peak wavelength (nm) as a function of the Au mole fraction in the starting Ag/Au powder mixture. Red, black, and blue circles indicate sample sets 1, 2, and 3, respectively. The green line is a linear fit to the data.

APS 0.8−1.5 μm, 99.96%) powders dispersed by vigorous stirring in 50 mL of a 0.05 M aqueous solution of sodium dodecyl sulfate (SDS; Aldrich, 99%). The SDS was used as a stabilizing agent to maintain the nanoparticles in a colloidal suspension. The second harmonic beam (532 nm) of a Nd:YAG laser (Spectra-Physics, Quanta Ray PRO-290) was used. The laser irradiation time, repetition rate, and fluence were 30 min, 30 Hz, and 590 (mJ/cm^2)/pulse, respectively. The raw colloidal suspensions were centrifuged (Cole-Parmer, no. 17250-10 centrifuge) for 15 min at 3400 rpm. The top 90% of the supernatant was collected for characterization and further use, while the precipitate containing excess metal powders was discarded.

Each sample was characterized by absorption (UV−vis) spectroscopy, transmission electron microscopy (TEM), and energy-dispersive X-ray (EDX) spectroscopy. The absorption spectra were recorded in the 200−800 nm range using a UV−vis spectrophotometer (Varian, Cary 3). The nanoparticle

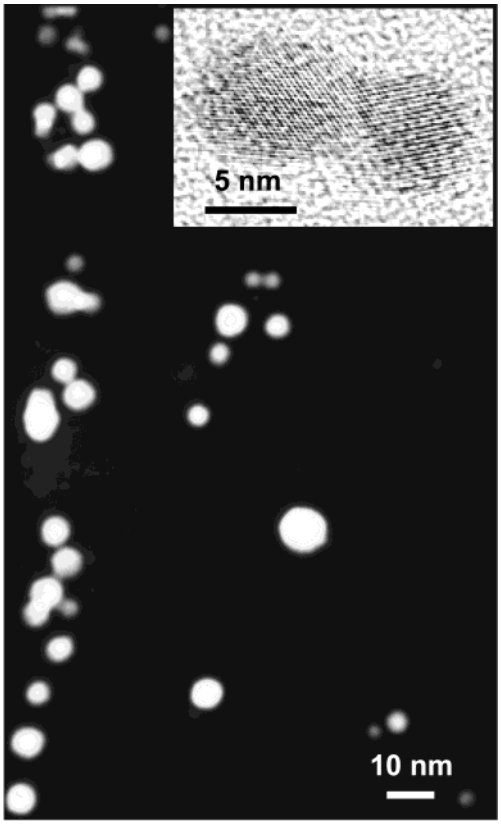

Figure 3. Annular dark field STEM image and HRTEM image (inset) of 1:1 Au−Ag nanoparticles from set 2.

samples were diluted ~1:20 in a 0.05 M solution of SDS in water for absorption spectrum measurement. The background due to the absorption in SDS/water solution was subtracted. Annular dark field (ADF) STEM and high-resolution (HR) TEM images and EDX spectra were obtained using a transmission electron microscope (JEOL, JEM-2010F). For the TEM measurements, a drop of a diluted sample was placed on a holey carbon copper grid and left to dry under an IR lamp.

III. Results

Three sets of experiments were carried out with the Au mole fraction in the starting Au/Ag powder mixtures equal to 0.1, 0.2, 0.3, 0.5, 0.6, 0.7, 0.8, and 0.9 in set 1, 0.0, 0.2, 0.4, 0.6, 0.8, and 1.0 in set 2, and 0.0, 0.25, 0.5, 0.75, and 1.0 in set 3. A photograph of the diluted Ag−Au colloids from set 1 is shown in the top panel of Figure 1. The gradual change of color with the changing Au:Ag ratio in the starting powder suspension is apparent. The corresponding UV−vis absorption spectra are shown in the bottom panel of Figure 1. The maximum of the plasmon resonance shifts gradually from 398 to 510 nm in parallel with the increasing Au mole fraction. The facts that the characteristic plasmon resonances for the pure Ag and Au nanoparticles (398 and 510 nm, respectively) are absent in the mixed-metal samples and that plasmon resonances below 398 nm and above 510 nm are not observed indicate that the resulting colloids contain Ag−Au alloyed nanoparticles rather than segregated metals, for example, core−shell-structured ones.[23] The absorption spectra were analyzed using the Drude model augmented with Lorentzian oscillators as recently applied by Moskovits et al.[23] The modelization reproduced the observed spectra within experimental error and proved the alloyed nature of the nanoparticles. The details of the analysis will be reported elsewhere.

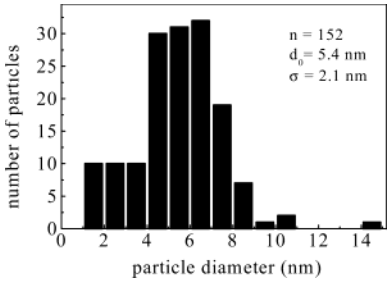

Figure 4. Size distribution of 1:1 Au−Ag nanoparticles from set 2. *n*, d_0, and σ denote the total number of measured particles, mean size (nm), and standard deviation (nm), respectively.

The wavelength of the plasmon resonance maximum increases approximately linearly with increasing Au mole fraction, as shown in Figure 2. The shift per unit mole fraction (1%) is equal to 1.1(1) nm/1% The scatter is due to experimental errors of sample weighing, inhomogeneity of the starting suspensions, and stirring problems. A similar linear relationship was obtained by Lee et al. for Au−Ag alloys produced by laser ablation.[19]

Further support for the homogeneous alloy structure of the Ag−Au nanoparticles has been provided by transmission electron microscopy. Figure 3 shows the ADF micrograph of the nanoparticles prepared with the 1:1 mixture of Ag and Au powders (set 2). The round nanoparticles appear homogeneous in composition since the sensitive ADF Z-atomic contrast is constant within the nanoparticles. High-resolution TEM (Figure 3, inset) also indicates that the nanoparticles are homogeneous since no apparent signs of core−shell structure or other segregation of metals are observed. The presence of fringes indicates that the Au−Ag nanoparticles are crystalline. Lattice spacings of ∼0.22, 0.20, and, occasionally, 0.14 nm have been measured. These values would correspond to the 111, 200, and 220 interplanar separation, respectively, for a 4.082 Å unit cell of an alloy of Au/Ag in equal proportion as estimated from Vegard's law. The size distribution of the nanoparticles in the 1:1 Ag−Au (set 2) has been determined from the analysis of 152 isolated nanoparticles in the ADF micrograph (see Figure 4). The distribution is centered at 5.4 nm with the standard deviation equal to 2.1 nm. Detailed analysis of a size distribution in the colloids with other than a 1:1 Ag−Au ratio is in progress. Preliminary results indicate that the mean diameter of the nanoparticles produced at the constant laser fluence increases with increasing Ag content, with the pure Au nanoparticles being the smallest and the pure Ag nanoparticles being the largest, about twice as large as the pure Au ones. The mean size variation can be compensated by accordingly increasing the laser fluence.

Finally, the strongest evidence for the homogeneous alloy structure of the nanoparticles comes from EDX spectroscopy of single isolated nanoparticles. A typical EDX spectrum, which shows a Ag−Au bimetallic composition of a nanoparticle, is presented in the lower panel of Figure 5. In Figure 6, an ADF STEM image of three nanoparticles from the 1:3 Ag−Au sample (set 3) is shown. The uniform intensity distribution (Z-atomic contrast) for each of the three nanoparticles rules out a core−shell or any other segregated metal structure. Slightly darker rings around the nanoparticles result form a shorter path of the probe beam through the particles near the edges. Superimposed in Figure 6 are Ag and Au traces (X-ray counts, arbitrary units) from a linear EDX scan across the three nanoparticles with a step of 0.5 nm, which show the distribution of the metals in a 0.5 nm thick slice of the nanoparticles. This is indisputable evidence for the homogeneous alloy structure of our nanoparticles. A detailed EDX investigation of the complete set of Ag−Au samples is presently in progress, and the results will be reported in a separate paper. In the upper panel of Figure 5, an EDX spectrum of a Co−Mo nanoparticle is shown. The Co−Mo nanoparticles were also produced by laser irradiation of a mixture of Co/Mo powders suspended in water with SDS as a stabilizing agent. This illustrates a versatility of the present method. It should be noted that, for some metal powders, including cobalt and molybdenum, formation of metal oxide nanoparticles is also possible. However, there is no evidence that this was the case in our experiment. Detailed characterization of the Co−Mo nanoparticles as well as several other types of metal alloy nanoparticles produced by the method described in this paper is presently under way.

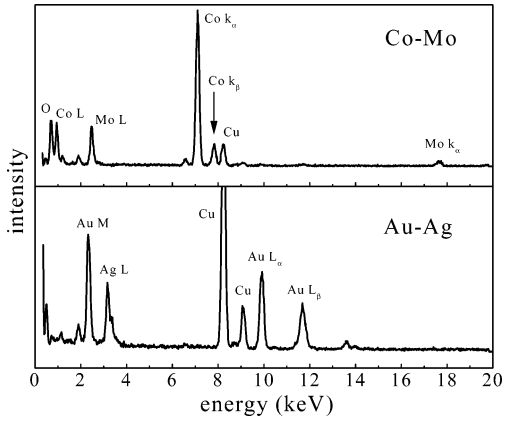

Figure 5. EDX spectra of an individual 1:1 Au−Ag nanoparticle from set 2 (bottom panel) and a 1:2 Co−Mo nanoparticle (top panel). Unassigned peaks originate from SDS or external contaminants (Fe, Si).

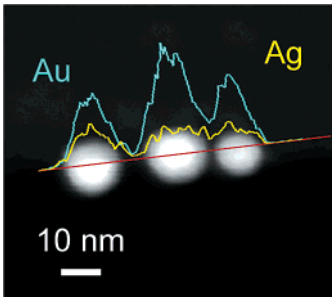

Figure 6. Annular dark field STEM images of three 1:3 Ag−Au nanoparticles (set 3). Linear EDX scan traces (X-ray counts, arbitrary units) for Ag (yellow) and Au (blue) are also shown superimposed on the ADF STEM images.

IV. Discussion

The method reported in this paper is applicable to various metal mixtures in SDS/water solution, as illustrated by the results for the Au−Ag and Co−Mo nanoparticles presented above. It is also applicable to nonaqueous solvents. For instance, Au−Ag nanoparticles have been produced in heptane and hexane and Co−Ni nanoparticles in toluene. In addition, early evidence suggests that Ru−Pt nanoparticles can be grown in ethylene glycol. The rate at which nanoparticles are formed appears to be solvent dependent. However, details of the dependence have not been investigated systematically. In the case where an aqueous medium works better but an organic phase is required, the nanoparticles can be transferred from the aqueous phase to the organic phase using the simple method reported by Gaponik et al. for semiconductor nanocrystals.[24] We verified that the method also works for SDS-stabilized metal nanoparticles. The

Ag−Au nanoparticles were extracted from the aqueous solution using dodecanethiol as both the organic solvent and stabilizer. A small amount of dodecanethiol (~2 cm^3) was added to the aqueous solution. The mixture was shaken vigorously and left for several minutes on the benchtop. The dodecanethiol and water phases separated within 10−15 min with water at the bottom of the sample tube and dodecanethiol-containing nanoparticles at the top. It was noted that very gentle heating sped up the extraction.

Formation of the nanoparticles is not well understood at present. The laser beam dissociates the micrometer-sized particles into smaller fragments, which through a recombination−dissociation cycle homogenize the nanoparticle composition. However, the mechanism of the micrometer-sized particle fragmentation by laser radiation remains unclear. Is it purely ablation/vaporization, or does some electron charging process mediated by the solvent followed by Coulomb separation cause the particles to disintegrate? Fragmentation of submicrometer-sized particles is much better understood. It was extensively studied by Kamat et al.[25] and Takami et al.[26] with pure noble metal nanoparticles. Kamat et al.[25] showed that irradiation of large Ag nanoparticles with a 355 nm laser beam leads to electron ejection and charging of the nanoparticle surface, which in turn result in disintegration of large particles and formation of smaller ones. Takami et al.[26] argued that fragmentation of large Au nanoparticles irradiated with a 532 nm laser beam results from a multistep process including boiling of the large particles, evaporation of atoms and small particles, and their subsequent agglomeration. Applicability of the above-described fragmentation mechanisms for metal alloy nanoparticles and micrometer-sized pure Ag and Au particles is addressed by experiments currently under way in our laboratory.

V. Conclusions

In this paper we showed that laser radiation can be used to prepare alloyed metal nanoparticles from suspensions of micrometer-sized metal powder mixtures. The method was demonstrated here for the Au−Ag and Co−Mo nanoparticles. Preliminary results indicate that it can also be applied to several other nanoparticle systems, including monometallic nanoparticles, in aqueous as well as various organic solvents. We expect that the method will be used in research laboratories whenever small amounts but a large variety of nanoparticles are required. We also believe that it will stimulate development of new chemical, biological, physical, and environmental applications.

References and Notes

(1) *Metal Nanoparticles. Synthesis, Characterization and Applications*; Feldheim, D. L., Foss, C. A., Eds.; Marcel Dekker: New York, 2002.
(2) Bruchez, M., Jr.; Mronne, M.; Gin, P.; Weiss, S.; Alivisatos, A. P. *Science* **1998**, *281*, 2013.
(3) Murray, C. B.; Norris, D. J.; Bawendi, M. G. *J. Am. Chem. Soc.* **1993**, *115*, 8706.
(4) Jin, R.; Cao, Y.-W.; Mirkin, C. A.; Kelly, K. L.; Schatz, G. C.; Zheng, J. G. *Science* **2001**, *294*, 1901.
(5) Kim, Y.; Johnson, R. C.; Hupp, J. T. *Nano Lett.* **2001**, *1*, 165.
(6) Elghanian, R.; Storhoff, J. J.; Mucic, R. C.; Letsinger, R. L.; Mirkin, C. A. *Science* **1997**, *277*, 1078.
(7) Taton, T. A.; Mirkin, C. A.; Letsinger, R. L. *Science* **2000**, *289*, 1757.
(8) Storhoff, J. J.; Elghanian, R.; Mucic, R. C.; Mirkin, C. A.; Letsinger, R. L. *J. Am. Chem. Soc.* **1998**, *120*, 1959.
(9) Park, S.-J.; Taton, T. A.; Mirkin, C. A. *Science* **2002**, *295*, 1503.
(10) Storhoff, J. J.; Lazarides, A. A.; Mucic, R. C.; Mirkin, C. A.; Letsinger, R. L.; Schatz, G. C. *J. Am. Chem. Soc.* **2000**, *122*, 4640.
(11) Mafune, F.; Kohno, J.-Y.; Takeda, Y.; Kondow, T. *J. Phys. Chem. B* **2001**, *105*, 9050.
(12) Mafune, F.; Kohno, J.-Y.; Takeda, Y.; Kondow, T. *J. Phys. Chem. B* **2002**, *106*, 7575.
(13) Mafune, F.; Kohno, J.-Y.; Takeda, Y.; Kondow, T.; Hisahiro, S. *J. Phys. Chem. B* **2001**, *105*, 5114.
(14) Mafune, F.; Kohno, J.-Y.; Takeda, Y.; Kondow, T.; Hisahiro, S. *J. Phys. Chem. B* **2000**, *104*, 9111.
(15) Mafune, F.; Kohno, J.-Y.; Takeda, Y.; Kondow, T.; Hisahiro, S. *J. Phys. Chem. B* **2000**, *104*, 8333.
(16) Simakin, A. V.; Voronov, V. V.; Shafeev, G. A.; Brayner, R.; Bozon-Verduraz, F. *Chem. Phys. Lett.* **2001**, *348*, 182.
(17) Kao, H.-M.; Wu, R.-R.; Chen, T.-Y.; Chen, Y.-H.; Yeh, C.-S. *J. Mater. Chem.* **2000**, *10*, 2802.
(18) Chen Y.-H.; Yeh, C.-S. *Colloids Surf., A* **2002**, *197*, 133.
(19) Lee, I.; Han, S. W.; Kim, K. *Chem. Commun.* **2001**, 1782.
(20) Chen Y.-H.; Yeh, C.-S. *Chem. Commun.* **2001**, 371.
(21) Chen, Y.-H.; Tseng, Y.-H.; Yeh, C.-S. *J. Mater. Chem.* **2002**, *12*, 1419.
(22) Yeh, M.-S.; Yang, Y.-S.; Lee, Y.-P.; Lee, H.-H.; Yeh, Y.-H.; Yeh, C.-S. *J. Phys. Chem. B* **1999**, *103*, 6851.
(23) Moskovits, M.; Srnova-Sloufova, I.; Vlckova, B. *J. Chem. Phys.* **2002**, *116*, 10435.
(24) Gaponik, N.; Talapin, D. V.; Rogach, A. L.; Eychmuller, A.; Weller, H. *Nano Lett.* **2002**, *2*, 803.
(25) Kamat, P. V.; Flumiani, M.; Hartland, G. V. *J. Phys. Chem. B* **1998**, *102*, 3123.
(26) Takami, A., Kurita, H., Koda, S. *J. Phys. Chem. B* **1999**, *103*, 1226.